JOURNAL OF GUIDANCE, CONTROL, AND DYNAMICS
Vol. 29, No. 3, May–June 2006

Satellite Collision Probability Enhancements

Salvatore Alfano*
Center for Space Standards and Innovation, Colorado Springs, Colorado 80920-6522

This work refines collision probability calculations for rectangular object shapes of unknown orientation and compares those results to their representations as spheres. Conjunction probability analysis for spherical objects exhibiting near-linear relative motion is accomplished by combining covariances and physical object dimensions at the point of closest approach. The resulting covariance ellipsoid and hardbody can then be projected onto the plane perpendicular to relative velocity. Collision potential is determined from the object's physical footprint on the projected, two-dimensional, probability density space. In the absence of object attitude information, a footprint that completely defines the region where the two objects might touch must be created. This footprint can then be rotated to determine the orientation that produces the largest probability making it the most conservative estimate for the given conjunction conditions. A further enhancement is presented to address the maximum possible probability for a given miss distance while also assessing the sufficiency of the orbital data to meaningfully support the calculations.

Nomenclature

AR	=	aspect ratio of major-to-minor projected covariance ellipse axes
C_{P_lo}	=	correspondence of the low, relative probability value
$dist$	=	distance of closest approach
ht	=	individual object height
lt	=	individual object length
OBJ	=	combined object radius
P	=	two-dimensional collision probability
$P_{\max}$	=	maximum collision probability
r_1	=	half-length of primary's largest dimension of projected rectangle
r_{1p}	=	half-width dimension perpendicular to half-length $r1$
r_2	=	half-length of secondary's largest dimension of projected rectangle
r_{2p}	=	half-width dimension perpendicular to half-length $r2$
w	=	combined object width factor
wt	=	individual object width
x	=	major axis direction
x_m	=	x component of projected miss distance
y	=	minor axis direction
y_m	=	y component of projected miss distance
α	=	orientation angle of distance vector
θ	=	orientation angle of projected object
σ_x	=	major axis standard deviation for combined covariance
σ_y	=	minor axis standard deviation for combined covariance
σ_{y0}	=	zero-order minor axis standard deviation approximation

Introduction

THERE is a growing body of work that addresses collision probability computations for neighboring space objects[1–12] and some literature that examines the associated accuracy requirements.[13,14] Typically, a determination is made when a secondary object transgresses a user-defined safety zone. The uncertainties associated with position are represented by three-dimensional Gaussian probability densities. At a given time, these densities take the form of covariance matrices and can be obtained from the owner-operators or independent surveillance sources such as the U.S. Space Object Catalog (Special Perturbations). Typically, positions and covariances are propagated to the time of closest approach, relative motion is assumed nearly linear,[12] and the positional covariances are assumed constant and uncorrelated for the encounter. Visually, the encounter region looks like a straight tube (collision tube) in three-dimensional space. For complex space structures, where the cross-section dimensions are small compared to the standard deviations or miss distance, Chan has developed an approximation technique known as the method of equivalent cross-section areas.[8]

Space object collision avoidance is usually conducted with the objects modeled as spheres. The combined covariance size, shape, and orientation are coupled with physical object sizes to determine collision potential. At the point of closest approach, each object's positional uncertainty is combined, and their radii summed. For linear relative motion, the resultant is projected onto a plane perpendicular to the relative velocity where the collision probability is calculated.[9] The projection reduces the probability formulation to a double integral that can be further simplified to a single integral through use of error functions.

The accuracy of positional covariance matrices resulting from least-squares orbit determination of sparse data is questionable. Covariance matrices formed in this manner often provide overly optimistic results. Foster and Frisbee[15] note "The primary problem with state error covariances determined from observations of objects in Earth orbit is that they are not truly reflective of the uncertainties in the dynamic environment." To address this concern, they devised a method to scale covariances provided to NASA by Air Force Space Command. This paper circumvents the inaccuracy of covariance matrices by determining the maximum probability for an encounter. Because all operational decisions are ultimately made with respect to the amount of acceptable risk, the goal is to shift the decisional comparison from a fixed positional threshold to the probability of the objects coming within a certain threshold. This is already done with the International Space Station and Space Transportation System, in which avoidance maneuvers are initiated if the collision probability exceeds an acceptable risk threshold. For a specified covariance aspect ratio, the maximum probability method guarantees an upper bound that will not be exceeded regardless of satellite positional uncertainty. The focus of this paper is to determine the maximum probability by examining the mean distance and the orientations of the physical satellites. If the maximum probability approach results in excessive maneuvers or unacceptable reductions in mission opportunity, then the true probability should be assessed if the data are deemed sufficiently accurate to support the calculation.

The first portion of this paper examines the computations for rectangular objects. Physical satellite dimensions can be obtained by owner/operators or assessed through observation. The subsequent

Presented as Paper 2004-5217 at the AIAA/AAS Astrodynamics Specialist Conference, Providence, RI, 16–19 August 2004; received 11 January 2005; revision received 20 April 2005; accepted for publication 20 April 2005.

*Technical Program Manager, AGI/CSSI, 7150 Campus Drive, Suite 260; salfano@centerforspace.com. Associate Fellow AIAA.

collision probability calculations can then be refined using knowledge of the rectangular object shapes and their orientations. The noncircular footprint is integrated over the projected covariance. The attitude must be considered because it changes the region of integration (footprint). Ideally, the attitude of each object should be known to accurately assess probability. For the more typical case where object orientation(s) are not known, this work shows how to create a footprint that completely defines the region where the two objects might touch. The relative position vector defines the footprint center; the footprint can then be rotated to determine the object orientation that produces the largest (most conservative) collision probability for the encounter holding all other parameters fixed.

This second portion of this paper builds on the first by showing how to determine the maximum collision probability. For a set of physical object dimensions, the covariance size and orientation are optimized while orienting the combined object footprint relative to the combined error ellipse. This method assumes the combined covariance shape is valid, but makes no assumption regarding the covariance size or orientation. The maximum collision probability establishes an upper bound associated with such scaling. An added benefit of this method is the ability to associate probability with risk. If the combined covariance size that maximizes probability is larger than the one used to assess true probability, the assessment can be associated with risk. If not, then more accurate positional data should be obtained.

Brief Review of Simplified Collision Probability Formulation

Numerous assumptions are made when computing collision probability for spherical objects with near-linear relative motion.[11] The relative motion is presumed essentially linear and the positional covariances of the two objects are considered independent and static over the conjunction time span of several seconds or less. The volume swept out by the secondary object becomes a cylinder extending along the relative velocity axis. The cylinder is of sufficient length to span tens of standard deviations, essentially making the one-dimensional probability unity along this axis. The relative velocity axis is associated with the time of the conjunction; a probability of one simply means the conjunction will take place. This axis can therefore be eliminated from consideration because the closest approach point occurs perpendicular to it. The hard-body radii are summed to form a combined object radius (OBJ), and the positional covariances are also summed. At the time of closest approach, a projection is done onto the plane perpendicular to relative velocity (often called the collision plane), thereby reducing the dimensional complexity from three to two. For convenience, the axes of the collision plane can be aligned to correspond with the major and minor axes of the projected, combined, error ellipse. The ellipse is formed from the summation, dimensional reduction, and rotation of the positional covariances. The standard deviations are represented as σ_x (major axis) and σ_y (minor axis). The projected relative position (x_m, y_m) in this two-dimensional space is then used to compute the cumulative collision probability P of collision from the equation:

$$P = \frac{1}{2 \cdot \pi \cdot \sigma_x \cdot \sigma_y} \cdot \int_{-OBJ}^{OBJ} \int_{-\sqrt{OBJ^2 - y^2}}^{\sqrt{OBJ^2 - y^2}} \exp\left\{\left(\frac{-1}{2}\right) \cdot \left[\left(\frac{x + x_m}{\sigma_x}\right)^2 + \left(\frac{y + y_m}{\sigma_y}\right)^2\right]\right\} \mathrm{d}x \times \mathrm{d}y \tag{1}$$

The aspect ratio AR is introduced as a multiple of the σ_y ($\mathrm{AR} \geq 1$) such that

$$P = \frac{1}{2 \cdot \pi \cdot \mathrm{AR} \cdot (\sigma_y)^2} \cdot \int_{-OBJ}^{OBJ} \int_{-\sqrt{OBJ^2 - y^2}}^{\sqrt{OBJ^2 - y^2}} \exp\left\{\left(\frac{-1}{2}\right) \cdot \left[\left(\frac{x + x_m}{\mathrm{AR} \cdot \sigma_y}\right)^2 + \left(\frac{y + y_m}{\sigma_y}\right)^2\right]\right\} \mathrm{d}x \times \mathrm{d}y \tag{2}$$

For the formulation that follows, Eq. (2) is rewritten as

$$P = \frac{OBJ^2}{2 \cdot \pi \cdot \mathrm{AR} \cdot (\sigma_y)^2} \cdot \int_{-1}^{1} \int_{-\sqrt{1 - y^2}}^{\sqrt{1 - y^2}} \exp\left\{\left(\frac{-1}{2}\right) \cdot \left[\left(\frac{x_m + x \cdot OBJ}{\mathrm{AR} \cdot \sigma_y}\right)^2 + \left(\frac{y_m + y \cdot OBJ}{\sigma_y}\right)^2\right]\right\} \mathrm{d}x \times \mathrm{d}y \tag{3}$$

Formulation for Collision Probability with Unknown Orientation and Linear Relative Motion

A two-dimensional rectangle can be formed from the three-dimensional hard-body object dimensions of height ht, width wd, and length lt such that all possible combinations of projection and attitude are completely captured. For the following analysis the dimensions are ordered so that $lt \geq wd \geq ht$. The all-encompassing rectangle has the dimensions shown in Fig. 1.

One-half of the diagonal for the rectangular solid object is denoted as r_1.

$$r_1 = \sqrt{(lt_1)^2 + (wd_1)^2 + (ht_1)^2}\big/2 \tag{4}$$

From geometrical considerations, the greatest half-width r_{1p} perpendicular to r_1 is

$$r_{1p} = lt_1 \cdot \sqrt{1 - [lt_1/(2 \cdot r_1)]^2} \tag{5}$$

Similarly, the half-length r_2 of the secondary object's largest projected rectangle dimension is

$$r_2 = \sqrt{(lt_2)^2 + (wd_2)^2 + (ht_2)^2}\big/2 \tag{6}$$

and the half-width r_{2p} perpendicular to r_2 is

$$r_{2p} = lt_2 \cdot \sqrt{1 - [lt_2/(2 \cdot r_2)]^2} \tag{7}$$

The combined object radius OBJ is defined as

$$OBJ = r_1 + r_2 \tag{8}$$

and the width factor w is

$$w = \frac{\min(r_{1p} + r_2, r_1 + r_{2p})}{OBJ} \tag{9}$$

Figure 2 shows the overlay of the projected rectangle on the projected circle. The combined object must be contained in both spaces, meaning the shaded areas can be eliminated.

Because the orientation of the resulting projection is unknown, it must now be rotated through an angle θ measured from the combined-covariance ellipse major axis. This is done to produce the largest collision probability for the given location (x_m, y_m) and associated, combined-covariance standard deviations (σ_x, σ_y) in the projected frame. As a function of θ, the probability equation takes

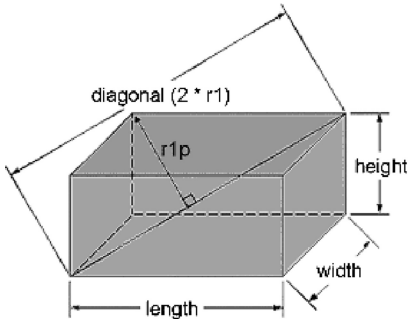

Fig. 1 Primary object projection geometry.

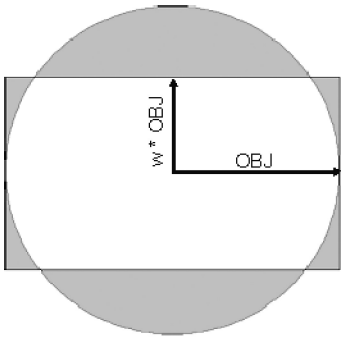

Fig. 2 Superposition of projected rectangle and circle.

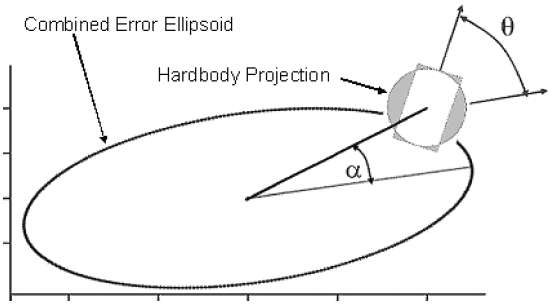

Fig. 3 Relationship of angles α and θ to major axis after projection onto notional collision plane.

the form

$$P = \frac{OBJ^2}{2 \cdot \pi \cdot \mathrm{AR} \cdot (\sigma_y)^2} \cdot \int_{-w}^{w} \int_{-\sqrt{1-y^2}}^{\sqrt{1-y^2}} \exp\left[\left(\frac{-1}{2}\right) \cdot \left(\left\{\frac{x_m + [x \cdot \cos(\theta) + y \cdot \sin(\theta)] \cdot OBJ}{\mathrm{AR} \cdot \sigma_y}\right\}^2 + \left\{\frac{y_m + [y \cdot \cos(\theta) - x \cdot \sin(\theta)] \cdot OBJ}{\sigma_y}\right\}^2\right)\right] \mathrm{d}x \times \mathrm{d}y \quad (10)$$

Equation (10) differs from Eq. (3) in two areas. The limits of y integration now reflect the rectangular nature of the objects. Also, the exponential expression is more complex because the combined object footprint reflected in Fig. 2, unlike the circle, is not universally symmetric.

Formulation for Maximum Collision Probability with Unknown Orientation and Linear Relative Motion

This formulation determines the worst-case conjunction scenario by finding the combined Gaussian error probability density function that maximizes collision probability. Small changes in the combined covariance can result in significant changes in the probability. In the absence of additional (more accurate) data or refinements in orbit determination, it is assumed that the general shape of the projected covariance ellipse is correct although its size and orientation might not be. A new angle α is introduced to define the orientation of the distance vector with respect to the covariance ellipse major axis. For a fixed miss distance, combined object size, and width factor, the projected covariance size and relative orientation are varied to produce the maximum collision probability while the covariance aspect ratio is held fixed. This is different from the preceding section, where the largest probability was found by varying θ while holding the covariance size σ_y and orientation α fixed. The angle α is illustrated in Fig. 3 along with the orientation angle of the projected object θ as measured from the ellipse's major axis.

The probability equation as a function of α, and θ becomes

$$P = \frac{OBJ^2}{2 \cdot \pi \cdot \mathrm{AR}(\sigma_y)^2} \cdot \int_{-w}^{w} \int_{-\sqrt{1-y^2}}^{\sqrt{1-y^2}} \exp\left[\left(\frac{-1}{2}\right) \times \left(\left\{\frac{dist \cdot \cos(\alpha) + [x \cdot \cos(\theta) + y \cdot \sin(\theta)] \cdot OBJ}{\mathrm{AR} \cdot \sigma_y}\right\}^2 + \left\{\frac{dist \cdot \sin(\alpha) + [y \cdot \cos(\theta) - x \cdot \sin(\theta)] \cdot OBJ}{\sigma_y}\right\}^2\right)\right] \mathrm{d}x \times \mathrm{d}y \quad (11)$$

The maximum collision probability occurs at the closest approach point when the relative position vector is aligned with the major axis of the combined covariance ellipse (α equals zero) coincident with the object's probability mass symmetrically distributed about the major axis (θ equals zero). It can readily be shown that under these conditions the first derivative with respect to each angle is zero and their second derivatives are negative. The maximum collision probability for a given covariance size σ_y and shape AR is therefore simplified to

$$P_{\max} = \frac{OBJ^2}{2 \cdot \pi \cdot \mathrm{AR} \cdot (\sigma_y)^2} \cdot \int_{-w}^{w} \int_{-\sqrt{1-y^2}}^{\sqrt{1-y^2}} \exp\left\{\left(\frac{-1}{2}\right) \cdot \left[\left(\frac{dist + x \cdot OBJ}{\mathrm{AR} \cdot \sigma_y}\right)^2 + \left(\frac{y \cdot OBJ}{\sigma_y}\right)^2\right]\right\} \mathrm{d}x \times \mathrm{d}y \quad (12)$$

With θ qualing zero to optimize the object orientation and α equaling zero to optimize the relative distance direction, the final step determines the size of the projected covariance that maximizes Eq. (12). The derivative of Eq. (12) is taken with respect to σ_y and the resulting exponential function in the integrand approximated to zeroth order. The resulting double integral is set equal to zero to determine the value of σ_y, which maximizes the probability. This zero-order approximation σ_{y0} becomes

$$\sigma_{y0} = \frac{OBJ}{2 \cdot \mathrm{AR}} \cdot \sqrt{\frac{\left[(1 - 3 \cdot \mathrm{AR}^2) \cdot w \cdot (\sqrt{1 - w^2})^3\right]}{3 \cdot \left[w \cdot \sqrt{1 - w^2} + \arcsin(w)\right]} + \left[\frac{(\mathrm{AR}^2 + 1)}{2} + 2 \cdot \left(\frac{dist}{OBJ}\right)^2\right]} \quad (13)$$

The value of the preceding expression can be used in Eq. (12) to initialize σy. Iteration on σy is then performed to find the maximum collision probability within the bounds of user tolerance.

If the combined object footprint contains the covariance ellipsoid center ($dist < OBJ$), the maximum probability approaches one as the standard deviation along the minor axis nears zero. This is the limiting case and must be independently addressed. The method described in this section only applies when the combined object does not encompass the covariance center ($dist \geq OBJ$). Given the combined object radius, width factor, and distance from center, the minor axis size can be determined by maximizing the preceding probability expression with respect to σ_y. Once determined, the worst-case collision probability is calculated.

The minor axis size that produces the maximum probability can also be used to determine if the positional data are sufficiently accurate to yield a meaningful collision probability assessment.[14] If it is larger than that of the original combined covariance, the true probability assessment can be associated with risk. If not, then more accurate positional data should be obtained, and both the true and maximum probability analysis redone.

Numerical Testing for Near-Linear Relative Motion

Approximately 500,000 test cases were used to evaluate the preceding probability expressions. These cases had all parameters normalized to the minor axis standard deviation. The object size varied from 10^{-3} to 10^{+3}, the miss distance varied from 10^{-4} to 10^{+3} with position ranging from 0 to 90 deg relative to the major axis (α), and

the aspect ratio varied from 1 to 50. Additionally, the object's orientation angle θ was varied from 0 to 180 deg relative to the major axis with the width factor ranging from 0.01 to 0.99. To understand the benefits of treating objects as rectangles, all results are given as a percentage of the collision probability for spherical objects. In the representative plots that follow, a solid line with diamonds indicates the mean relative probability, a dashed line with x symbols represents the maximum relative probability, and a dotted line with circles represents the minimum relative probability. All computations were done using MATHCAD 11 set to the highest tolerance (10^{-11}) that would still allow convergence of the integrals.

Figures 4 and 5 show the characteristic behavior of the collision probability function with respect to the width factor. The correspondence of the mean relative probability to the width factor is not one to one; halving the width factor does not produce half the probability. When the combined object radius is less than the relative distance, the mean and minimum values are somewhat close in value as reflected in Fig. 4. The rectangular-to-spherical correspondence $C_{P\perp \mathrm{lo}}$ of the lowest relative probability values (represented by dotted line with circles) can be approximated by

$$C_{p\perp \mathrm{lo}} \cong \left\{2 \cdot \left[w \cdot \sqrt{1-w^2} + \arcsin(w)\right]\right\}/\pi \qquad (14)$$

The preceding equation is a simple indicator of what improvement can be reasonably expected when using a rectangular shape instead of a spherical one. The comparisons of the approximation to mean and minimum, relative probability values, are shown in Fig. 6. Only two lines appear in the figure because the approximation (represented by plus signs) is very close to the minimum (represented by circles).

The maximum collision probability expression was evaluated in a similar manner. The object radius was smaller than or equal to the miss distance, and no limit was set on the standard deviation. The object's orientation angle θ and relative distance angle α were fixed at zero with all other parameters varied as already mentioned. As before, all results are given as a percentage of the maximum collision probability for spherical objects. The legend description for the following figure also remains the same as does the MATHCAD 11 convergence tolerance.

Figures 7–10 show the characteristic behavior of the maximum collision probability function with respect to the width factor and aspect ratio. The standard deviation that produces the maximum

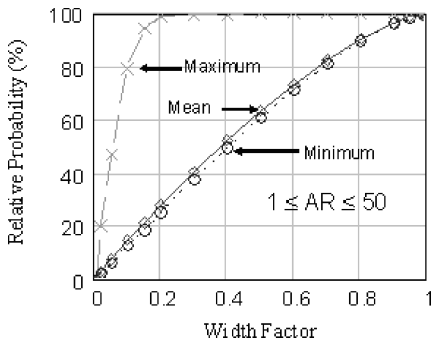

Fig. 4 Relative probability (*OBJ* < *dist*).

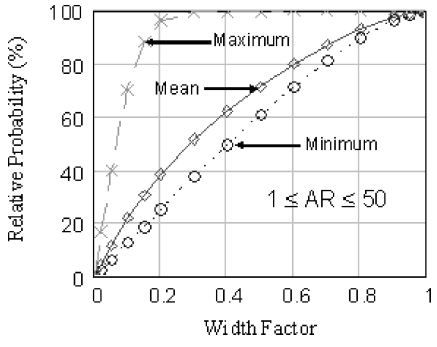

Fig. 5 Relative probability (*OBJ* ≥ *dist*).

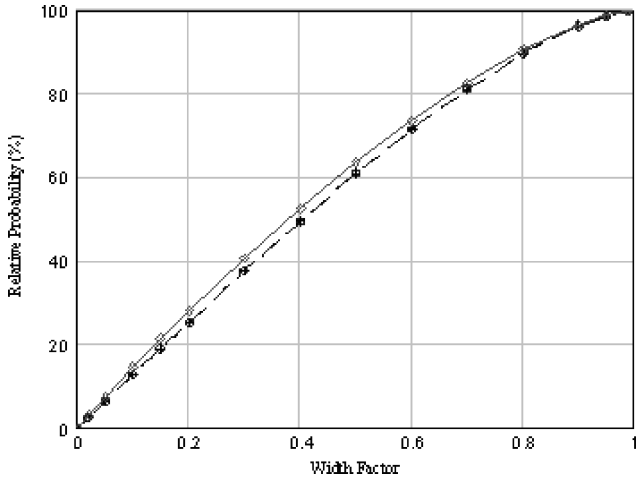

Fig. 6 Relative probability approximation comparison (*OBJ* < *dist*).

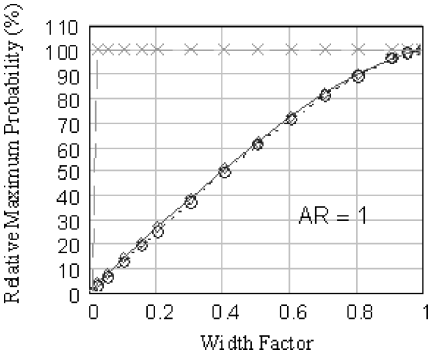

Fig. 7 Relative max probability (AR = 1).

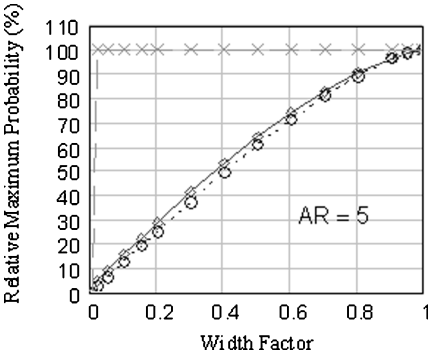

Fig. 8 Relative max probability (AR = 5).

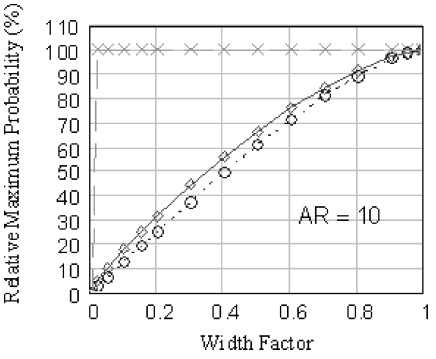

Fig. 9 Relative max probability (AR = 10).

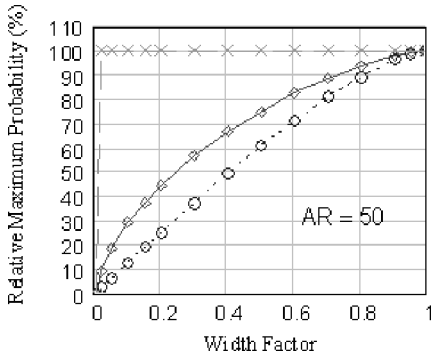

Fig. 10 Relative max probability (AR = 50).

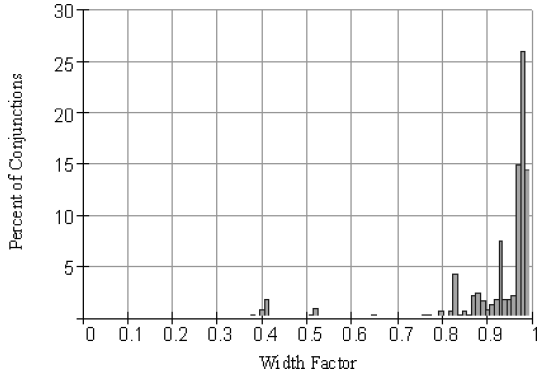

Fig. 11 Width factor histogram.

probability decreases as the width factor decreases. If the standard deviation is unconstrained and the object radius approaches the miss distance in value, the probability density becomes more concentrated near the origin. This has a two-fold effect as seen in the figures. The most obvious effect is that the greatest relative maximum probability (dashed line with x symbols) approaches 100% rapidly. The second effect is that the mean relative values (solid line with diamonds) also tend to be greater as the aspect ratio grows.

It is beneficial to get a sense of the width factor's variability. Every day that new NORAD two-line element sets are publicly released, a maximum conjunction probability report is generated and posted as a free advisory service at the website http://celestrak.com/SOCRATES/. The 29 June 2004 data were used to determine all object pairings of primaries (2627) with secondaries (8411) within 10 km for a seven-day span. The width factor for each of the resulting 26,752 pairs was then computed and binned to produce the histogram in Fig. 11, which clearly indicates the variability.

Summary

Conservative expressions were derived for the true and maximum conjunction probabilities of rectangular objects in the absence of attitude information. These expressions are important given the questionable accuracy of covariance matrices as of this writing. As expected, probability decreased when the rectangular nature was incorporated as opposed to assuming spherical satellite shapes. By simply examining the minor axis before and after maximum probability computations, one can determine if the positional data are sufficiently accurate to yield a meaningful collision probability assessment or if better data are needed. The results were based on the assumption that the encounter was of short duration (no more than several seconds) and that the data were Gaussian and representative of positional distribution at the time of closest approach. An approximation to mean probability relative to that of a spherical object was also given. A width-factor histogram for a single run of Satellite Orbital Conjunction Reports Assessing Threatening Encounters in Space (SOCRATES) was provided to give the reader a snapshot of variability. These methods can be used in cascading filters to determine if the risk of collision is sufficiently low to dismiss further computations.

References

[1]Foster, J. L., and Estes, H. S., "A Parametric Analysis of Orbital Debris Collision Probability and Maneuver Rate for Space Vehicles," NASA JSC 25898, Aug. 1992.

[2]Khutorovsky, Z. N., Boikov, V., and Kamnesky, S. Y., "Direct Method for the Analysis of Collision Probability of Artificial Space Objects in LEO: Techniques, Results, and Applications," *Proceedings of the First European Conference on Space Debris*, ESA SD-01, ESA, Paris, 1993, pp. 491–508.

[3]Carlton-Wippern, K. C., "Analysis of Satellite Collision Probabilities due to Trajectory and Uncertainties in the Position/Momentum Vectors," *Journal of Space Power*, Vol. 12, No. 4, 1993, pp. 349–364.

[4]Chan, K. F., "Collision Probability Analyses for Earth Orbiting Satellites," *Advances in the Astronautical Sciences*, Vol. 96, July 1997, pp. 1033–1048.

[5]Berend, N., "Estimation of the Probability of Collision Between Two Catalogued Orbiting Objects," *Advances in Space Research*, Vol. 23, No. 1, 1999, pp. 243–247.

[6]Oltrogge, D., and Gist, R., "Collision Vision Situational Awareness for Safe and Reliable Space Operations," International Astronautical Congress, Paper IAA-99-IAA.6.6.07, Oct. 1999.

[7]Akella, M. R., and Alfriend, K. T., "Probability of Collision Between Space Objects," *Journal of Guidance, Control, and Dynamics*, Vol. 23, No. 5, 2000, pp. 769–772.

[8]Chan, K. F., "Improved Analytical Expressions for Computing Spacecraft Collision Probabilities," American Astronautical Society, Paper 03-184, Feb. 2003.

[9]Patera, R. P., "General Method for Calculating Satellite Collision Probability," *Journal of Guidance, Control, and Dynamics*, Vol. 24, No. 4, 2001, pp. 716–722.

[10]Patera, R. P., "Satellite Collision Probability for Nonlinear Relative Motion," *Journal of Guidance, Control, and Dynamics*, Vol. 26, No. 5, 2003, pp. 728–733.

[11]Chan, K. F., "Spacecraft Collision Probability for Long-Term Encounters," *Advances in the Astronautical Sciences*, Vol. 116, No. 1, 2003, pp. 767–784.

[12]Chan, K. F., "Short-Term vs Long-Term Spacecraft Encounters," AIAA Paper 2004-5460, Aug. 2004.

[13]Gottlieb, R. G., Sponaugle, S. J., and Gaylor, D. E., "Orbit Determination Accuracy Requirements for Collision Avoidance," American Astronautical Society, AAS 01-181, Feb. 2001.

[14]Alfano, S., "Relating Position Uncertainty to Maximum Conjunction Probability," *Advances in the Astronautical Sciences*, Vol. 116, No. 1, 2003, pp. 757–766.

[15]Foster, J. L., and Frisbee, J. H., "Positional Error Covariance Matrix Scaling Factors for Early Operational ISS Debris Avoidance," NASA JSC DM33, 30 May 1998.